Journal of Photochemistry and Photobiology A: Chemistry 223 (2011) 1–5

Contents lists available at ScienceDirect

Journal of Photochemistry and Photobiology A: Chemistry

journal homepage: www.elsevier.com/locate/jphotochem

Observation of anthracene excimer fluorescence at very low concentrations utilizing dendritic structures

Ryosuke Akatsuka[a], Atsuya Momotake[a], Yoshihiro Shinohara[b], Yoko Kanna[c], Tomoo Sato[a], Masaya Moriyama[d], Kayori Takahashi[e], Yoshinobu Nishimura[a], Tatsuo Arai[a,*]

[a] Graduate School of Pure and Applied Sciences, University of Tsukuba, Tsukuba, Ibaraki 305-8571, Japan
[b] Research Facility Center for Science and Technology, University of Tsukuba, Japan
[c] Faculty of Science, University of the Ryukyus, Nishihara, Okinawa 903-0213, Japan
[d] Department of Applied Chemistry, Faculty of Engineering, Oita University, Oita 870-1192, Japan
[e] National Institute of Advanced Industrial Science and Technology (AIST), Tsukuba City, Ibaraki 305-8565, Japan

ARTICLE INFO

Article history:
Received 18 April 2011
Received in revised form 13 June 2011
Accepted 15 July 2011
Available online 30 July 2011

Keywords:
Anthracene
Dendrimers
Self-aggregations
Excimer emission

ABSTRACT

We prepared water-soluble anthracene-cored poly(aryl ether) dendrimers **wG1** and **wG2**, together with lipophilic dendrimers **G1** and **G2**, and examined their photochemical properties. Water-soluble dendrimers **wG1** and **wG2** produced excimer emissions peaking at 463 nm and 447 nm, respectively, in water at a concentration of 10^{-5} M, indicating that these dendrimers could form aggregates under highly diluted conditions. The results presented here are the first clear report of the observations of the excimer emission of anthracene in very low fluid solutions in which appropriate substituents were introduced.

1. Introduction

Dendrimers are supramolecules possessing well-defined, repeating units and a central core [1–4]. When the cone-shaped dendrimers [5–7], having hydrophilic surfaces with hydrophobic cores and branching units, are dissolved in water, self-aggregation to form a micelle-like structures occurs. In this case, the generation effect of the dendrimers on the aggregate formation is of interest. We have already prepared cone-shaped, water-soluble dendrimers of polyaromatic hydrocarbons such as pyrene that showed excimer emission due to the formation of aggregates of the core even at low concentrations of approximately 10^{-5} M [8]. Thus, water-soluble fluorescent molecules may give aggregates with characteristic fluorescences at longer wavelengths in contrast to the monomer emissions. In the case of naphthalene, researchers have observed excimer fluorescence in the solid state [9], polymers [10,11], photodimers [12], and dendrimers having several naphthalene chromophores at the periphery [13]; however the excimer fluorescence by intermolecular interaction in a very dilute solution could be observed only by use of cone-shaped dendrimer [14].

While pyrene and naphthalene have singlet lifetimes as long as 400 ns and 100 ns, respectively, in non-polar solvents and can easily form dimers or intermolecular aggregated forms within the lifetime of their singlet excited states, anthracene does not easily form intermolecular excimers because of the relatively short lifetime (4 ns) of its excited singlet state. Therefore, we attempted to observe the anthracene excimer at very low concentrations using cone-shaped dendrimers (Fig. 1).

Although anthracene-cored dendrimers have been prepared [15–17] where photochemical intermolecular dimerization reaction was observed [18,19], the anthracene excimer fluorescence in dilute aqueous solutions has not been reported thus far. We report a photochemical study on the generation and concentration-dependent aggregation of anthracene dendrimers in aqueous solution. The excimer fluorescence of anthracene was observed at concentrations as low as 2.0×10^{-5} M.

2. Experimental

2.1. Materials

2.1.1. 9-(3′,5′-Dihydroxyphenoxymethyl)anthracene (*1*)

A solution of 9-(bromomethyl)anthracene (1.00 g, 3.72 mmol) in 50 mL of DMF was added dropwise to a mixture of phloroglucinol (900 mg, 7.13 mmol) and K_2CO_3 (1.49 g, 10.7 mmol) in 10 mL

* Corresponding author. Tel.: +81 298 853 4315; fax: +81 298 853 6503.
E-mail address: arai@chem.tsukuba.ac.jp (T. Arai).

1010-6030/$ – see front matter © 2011 Published by Elsevier B.V.
doi:10.1016/j.jphotochem.2011.07.008

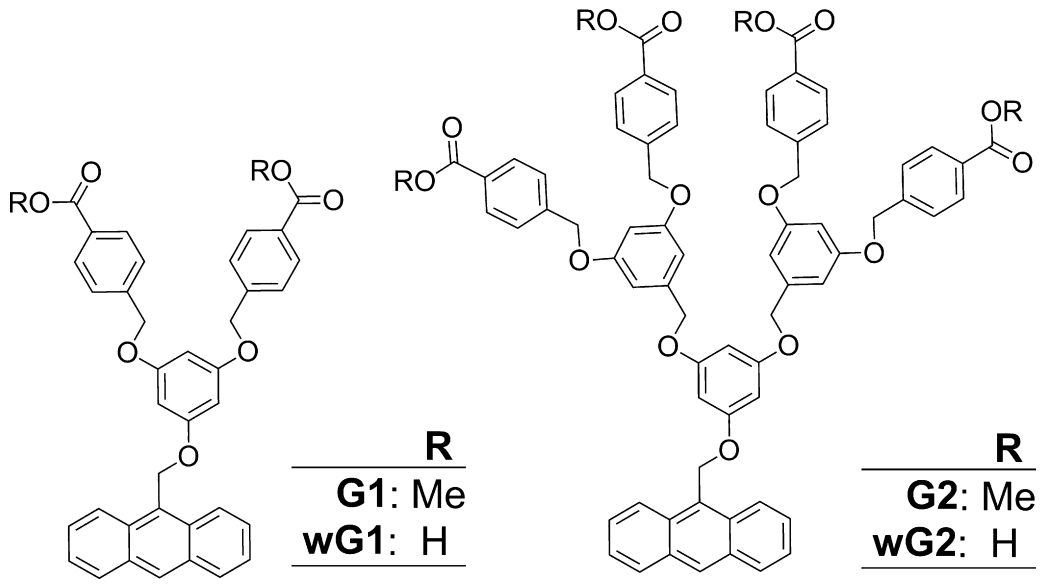

Fig. 1. Chemical structures of anthracene dendrimers.

of DMF, and the mixture was stirred for 6 h at room temperature under N_2. After evaporation to remove the solvent, water was added, and the resulting precipitate, including the desired product, was filtered and purified via silica gel column chromatography (dichloromethane/ether = 9/1) to give **1** as a pale yellow solid (177 mg) in a 15% yield.

^{1}H NMR (270 MHz, acetone-d6) δ 8.65 (1H, s), 8.43 (2H, d, J = 8.6 Hz), 8.13 (2H, d, J = 7.6 Hz), 7.50–7.63 (4H, m), 6.20 (2H, d, J = 2.1 Hz), 6.10 (1H, t, J = 2.1 Hz), 5.96 (2H, s).

2.1.2. G1 (Typical procedure)

A solution of **1** (0.150 g, 0.473 mmol) in 10 mL of THF was added to a mixture of 18-crown-6-ether (66 mg, 0.25 mmol), K_2CO_3 (287 mg, 2.1 mmol), methyl *p*-hydroxybenzoate (254 mg, 1.10 mmol) in 10 mL of acetone, and was stirred at 60 °C for 18 h. The solvent was evaporated after the resulting salts were filtered. The residue was purified via silica gel column chromatography (dichloromethane/ether = 9/1) followed by GPC (chloroform) to give **G1** as a white solid (118 mg) in a 39% yield.

^{1}H NMR (270 MHz, DMSO-d6) δ 8.49 (1H, s), 8.23 (2H, d, J = 8.4 Hz), 7.99–8.04 (6H, m), 7.44–7.54 (8H, m), 6.41 (3H, d, J = 2.0 Hz), 6.28 (1H, t, J = 2.0 Hz), 5.88 (2H, s), 5.04 (4H, s), 3.90 (6H, s); ^{13}C NMR (67.5 MHz, DMSO-d6) δ 166.8, 161.2, 160.5, 142.0, 131.5, 131.1, 130.1, 130.0, 129.2, 129.2, 127.0, 126.7, 126.6, 125.1, 124.0, 95.2, 95.1, 69.6, 63.0, 52.3;MALDI–TOF–MS (*m*/*z*) calcd. for $C_{39}H_{32}O_7$ $[M + Na]^+$ = 635.65; found, 634.92.

G2 was obtained by the same procedure in a 43% yield (250 mg).

^{1}H NMR (270 MHz, DMSO-d6) δ 8.52 (1H, s), 8.27 (2H, d, J = 8.6 Hz), 7.98–8.04 (10H, m), 7.44–7.53 (12H, m), 6.66 (4H, d, J = 2.16 Hz), 6.53 (2H, t, J = 2.16 Hz), 6.41 (2H, d, J = 1.9 Hz), 6.28

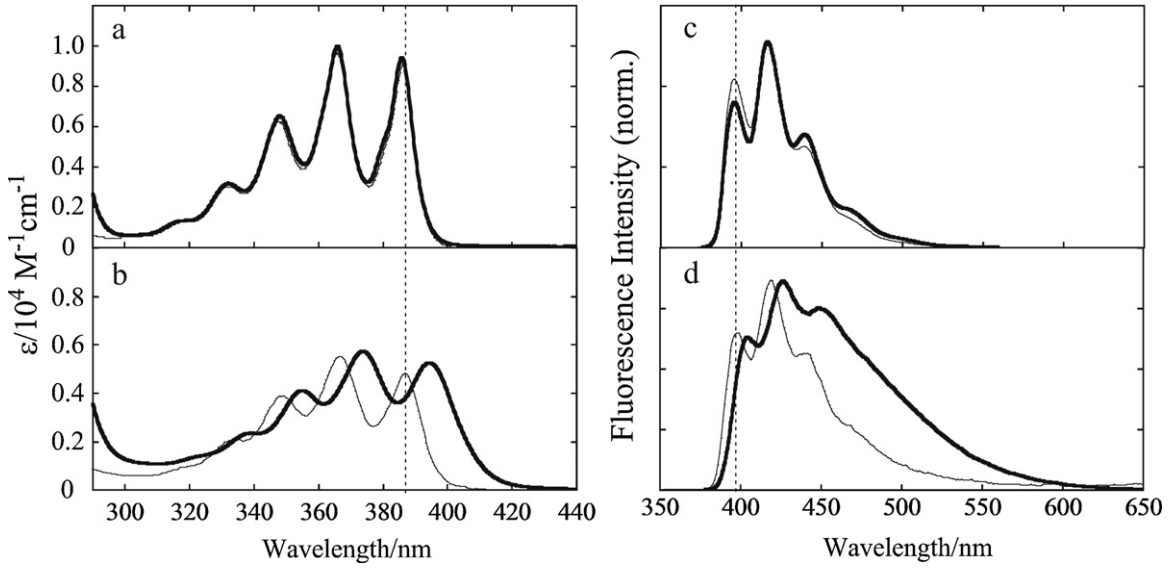

Fig. 2. (a) Steady state UV absorption spectra of **G1** (thin line) and **G2** (solid line) in THF. (b) Those of **wG1** (thin line) and **wG2** (solid line) in 0.1 M KOH aq. (c) Steady state fluorescence spectra of **G1** and **G2** in THF and (d) those of **wG1** and **wG2** in 0.1 M KOH aqueous solution. The excitation wavelength was 350 nm for all the experiments.

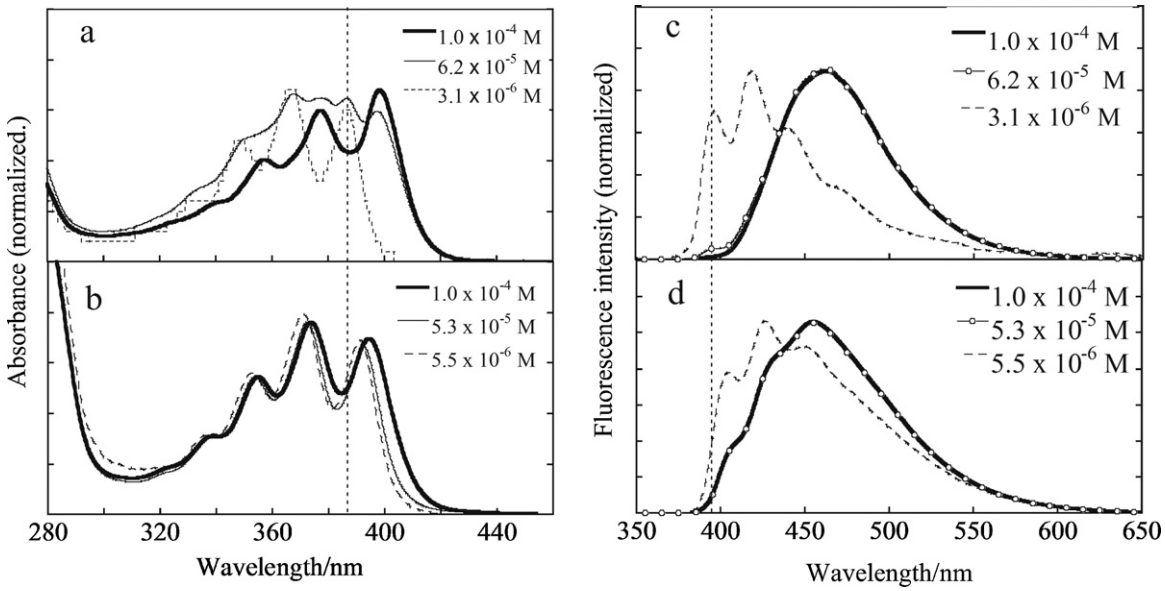

Fig. 3. Concentration dependence of the absorption spectra for (a) **wG1** and (b) **wG2**, and that of the fluorescence spectra for (c) **wG1** and (d) **wG2** in 0.1 M KOH aq.

(1H, m), 5.92 (2H, m), 5.09 (8H, s), 4.95 (4H, s), 3.90 (12H, s); MALDI–TOF–MS (*m*/*z*) calcd. for $C_{71}H_{60}O_{15}$ $[M+Na]^+$ = 1175.89; found, 1175.87.

2.1.3. wG1 (Typical procedure)

A solution of **G1** (135 mg, 0.223 mmol) in 14 mL of mixed solvent (1 M KOH/THF/MeOH = 1/12/2) was stirred at 60 °C for 8 h. A mixture was then acidified by the addition of 1 M HCl. The resulting precipitate was filtered and washed with distilled water to give **wG1** as a pale yellow solid (122 mg) in a 93% yield.

^{1}H NMR (270 MHz, DMSO-d6) δ 8.71 (1H, s), 8.33 (2H, d, J = 8.2 Hz), 8.15 (2H, d, J = 8.2 Hz), 7.95 (4H, d, J = 8.2 Hz), 7.63–7.53 (9H, m), 6.50 (2H, s), 6.38 (1H, s), 6.02 (2H, s), 5.17 (4H, s). ^{13}C NMR (67.5 MHz, DMSO-d6) δ 166.8, 160.5, 159.8, 141.8, 130.8, 130.3, 130.0, 129.3, 128.8, 128.4, 127.2, 127.0, 126.5, 125.1, 124.0, 94.9, 94.8, 68.8, 62.3; MALDI–TOF–MS (*m*/*z*) calcd. for $C_{37}H_{28}O_7$ $[M+Na]^+$ = 607.16; found, 607.33.

wG2 (89 mg) was obtained by the same procedure in a 78% yield.

^{1}H NMR (270 MHz, DMSO-d6) δ 8.80 (2H, d, J = 8.6 Hz), 8.58 (1H, s), 8.27–7.86 (12H, m), 7.49–7.44 (12H, m), 6.70 (4H, s), 6.61 (2H, s), 6.42 (2H, s), 6.29 (1H, s), 5.98 (2H, s), 5.11 (8H, s), 4.97 (4H, s); MALDI–TOF–MS (*m*/*z*) calcd. for $C_{67}H_{52}O_{15}$ $[M+Na]^+$ = 1096.33; found, 1096.72.

2.2. Measurements

We measured the ^{1}H NMR spectra with a JEOL EX-270 (270 MHz for ^{1}H NMR) or a Bruker ARX-400 (400 MHz for ^{1}H NMR) spectrometer in a solution of DMSO-d_6 with tetramethylsilane as an internal standard. The UV absorption and fluorescence spectra were recorded on a Shimadzu UV-1600 spectrophotometer and a Hitachi F-4500 fluorescence spectrometer, respectively. Fluorescence decay measurement was performed by time-correlated single photon counting method reported previously [20]. The time resolution is 20 ps.

3. Results and discussion

3.1. Steady state absorption and fluorescence spectra

3.1.1. Generation dependence

Table 1 summarizes the photochemical properties of anthracene dendrimers. All measurements were performed under argon at room temperature. The spectral shapes and the values of the molar extinction coefficients of **G1** and **G2** in THF were very similar to each other (Fig. 2a), suggesting that the substituted dendron did not provide the "generation effect" either electronically or sterically. The absorption spectra showed vibrational structures, and the peak of the lowest absorption band appeared at 386 nm for all lipophilic dendrimers. Fig. 2b shows the absorption spectra of the water-soluble analogs **wG1** and **wG2** in a 0.1 M KOH aqueous solution. In this case, the absorption band broadened and red shifted more significantly in higher generation. In addition, the molar extinction coefficients of the anthracene sites in **wG1** and **wG2** were less than that of **G1** and **G2**, probably due to the formation of aggregate even at a concentration lower than 10^{-5} M.

The fluorescence spectra of lipophilic dendrimers **G1** and **G2** in THF exhibited similar profiles and intensities, peaking around 396, 417, and 440 nm with the edges at 525 nm, which was assigned to the anthracene monomer emission (Fig. 2c). The water-soluble dendrimer **wG1** exhibited a slightly higher intensity at longer wavelengths, indicating the contribution of excimer-like emission at longer wavelengths. This observation was more pronounced in **wG2** because we observed the broad fluorescence up to 600 nm, accompanied by vibrational structures peaking at 402, 426, and

Table 1
Absorption and fluorescence maxima and fluorescence quantum yield for anthracene dendrimers.

	λ_{abs}/nm	ε/M^{-1} cm^{-1}	λ_{FL}/nm	Φ_f
G1	348, 366, 386	9600	396, 416, 439	0.16
G2	347, 365, 386	10,000	395, 416, 439	0.11
wG1	348, 366, 386	5500	398, 418, 440	0.067
wG2	352, 373, 391	4100	402, 426, 446	0.097

Table 2
Fluorescence lifetimes of **wG1** and **wG2** at various concentrations in 0.1 M KOH aq with excitation at 375 nm.

	Concentration/M	τ_s (at 430 nm)/ns (population (%))
wG1	3.1×10^{-6}	0.02 (84), 0.62 (14), 5.9 (2)
	6.2×10^{-5}	0.34 (20), 9.4 (80)
wG2	3.2×10^{-6}	0.27 (70), 3.0 (26), 16.1 (4)
	5.3×10^{-5}	0.31 (64), 3.9 (28), 19.4 (8)

446 nm (Fig. 2d). We ascribed the broadened fluorescence band to the anthracene excimer.

3.1.2. Concentration dependence

Fig. 3 shows the superposition of normalized spectra at varying concentrations. Both the absorption and the fluorescence spectra of **wG1** in aqueous solution (Fig. 3a and c) dramatically changed with increasing concentration. At low concentrations (3.1×10^{-6} M), **wG1** exhibited absorption and fluorescence bands similar to those of the lipophilic dendrimer whereas the absorption spectra at higher concentrations (10^{-4} M) was totally different (Fig. 3a). We attributed these results to the anthracene aggregation in the ground state. The emission band also broadened and red shifted at 10^{-4} M (Fig. 3c), assigned to the anthracene excimer. Interestingly, the concentration dependence of the higher generation **wG2** was different than that of **wG1**. The normalized absorption spectrum at 10^{-4} M was not very different from that at 5.5×10^{-6} M (Fig. 3b) because **wG2** formed aggregates even at a lower concentration (5.5×10^{-6} M) in which the anthracene unit partially existed as a monomer within the aggregates and the phenomenon did not significantly change by increasing the concentration. The fluorescence spectrum of **wG2** (Fig. 3d) at a low concentration (5.5×10^{-6} M) was probably the sum of the emission from the excited monomer and the excimer. At a high concentration (10^{-4} M), the fluorescence spectrum slightly broadened and red shifted, but we still observed weak vibrational structures at 405 and 427 nm, supporting our deduction that the excited monomer and excimer existed within the aggregates and that the population of the excimer increased at higher concentrations. The peak wavelengths and the spectral shapes of the anthracene excimer emission strongly depend on the manner of overlapping of the anthracene ring as described below.

Table 2 lists the fluorescence lifetimes of **wG1** and **wG2** in aqueous solution at different concentrations. We analyzed the lifetimes at low concentrations via multi-component analysis, which suggested a complicated aggregation structure and/or a partially monodispersed **wG1** and **wG2.** At higher concentrations, the longer lifetime component with $\tau_s = 9.4$ ns, probably due to the excimer emission produced by excitation of aggregated form, was dominant for **wG1** whereas the still fitted value of the multi-component of **wG2** supported a complicated formation of aggregate. The shorter lifetime components of which the population decreased with increasing dendrimer concentration can be assigned to the monomer fluorescence. The lifetime of excimer emission varies in different concentration or dendrimer generation because it may be dependent of the excimer structure.

Table 3
Fluorescence lifetimes of **wG1** (2.0×10^{-5} M) and **wG2** (2.0×10^{-5} M) at various concentrations in 0.001 M KOH aq with excitation at 375 nm.

	Concentration of KCl/mM	τ_s (at 430 nm)/ns (population (%))
wG1	0	0.08 (58), 0.87 (40), 5.3 (2)
	800	9.3 (100)
wG2	0	0.93 (43), 3.0 (51), 7.1 (6)
	800	1.3 (34), 3.8 (63), 10.1 (3)

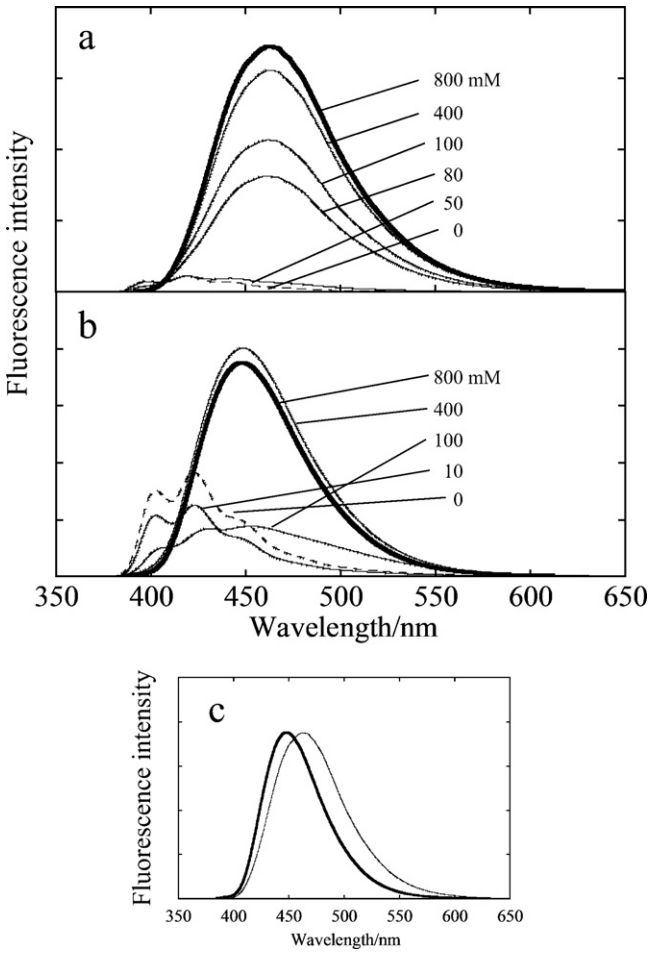

Fig. 4. Change in the fluorescence spectra upon the addition of KCl for (a) **wG1** (2.0×10^{-5} M) and (b) **wG2** (2.0×10^{-5} M) in 0.001 M KOH aqueous solution. (c) Comparison of the spectra of **wG1** and **wG2** in the presence of 800 mM KCl. The excitation wavelength was 350 nm for all the experiments.

3.1.3. Effective formation of aggregate via KCl addition

The addition of KCl could also induce aggregation of **wG1** and **wG2** in water, because the masking a carboxylate anion at the dendrimer periphery by added counterions (K^+) would reduce charge repulsion between dendrimers. In this case, we used 0.001 M KOH solutions instead of the 0.1 M KOH solution to observe the salt effect more clearly. Fig. 4a shows the change in the fluorescence spectra of **wG1** upon the addition of KCl wherein the excimer fluorescence dramatically increased with increasing KCl concentration. The fluorescence spectra of **wG2** also changed in a similar manner: a decrease of the monomer fluorescence at 402 nm and a simultaneous increase of the excimer fluorescence at 448 nm were observed (see Fig. 4b). Interestingly, the excimer fluorescence of **wG1** ($\lambda_{max} = 463$ nm) and **wG2** ($\lambda_{max} = 447$ nm) at high KCl concentrations did not overlap (see Fig. 4c), indicating that the excimer structure of **wG2** was different from that of **wG1**. Researchers have reported the structural dependence of the anthracene excimer for a variety of anthracenophane and bisanthrylethane [21] and 1-(1-anthryl)-3-(9-anthryl)propane (1,9-DAP, ($\lambda_{max} = 520$ nm)) and 1-(1-anthryl)-3-(2-anthryl)propane (1,2-DAP, ($\lambda_{max} = 470$ nm)) [22]. According to the results, the anthracene excimer can exist in a variety of geometries, and each one can have a different stability, emitting fluorescence over a range of 460–620 nm. Waldeck et al. deduced that the overlap of one of the phenyl rings in anthracene resulted in the excimer emission peaking around 460 nm, and the overlap of two or three of the phenyl

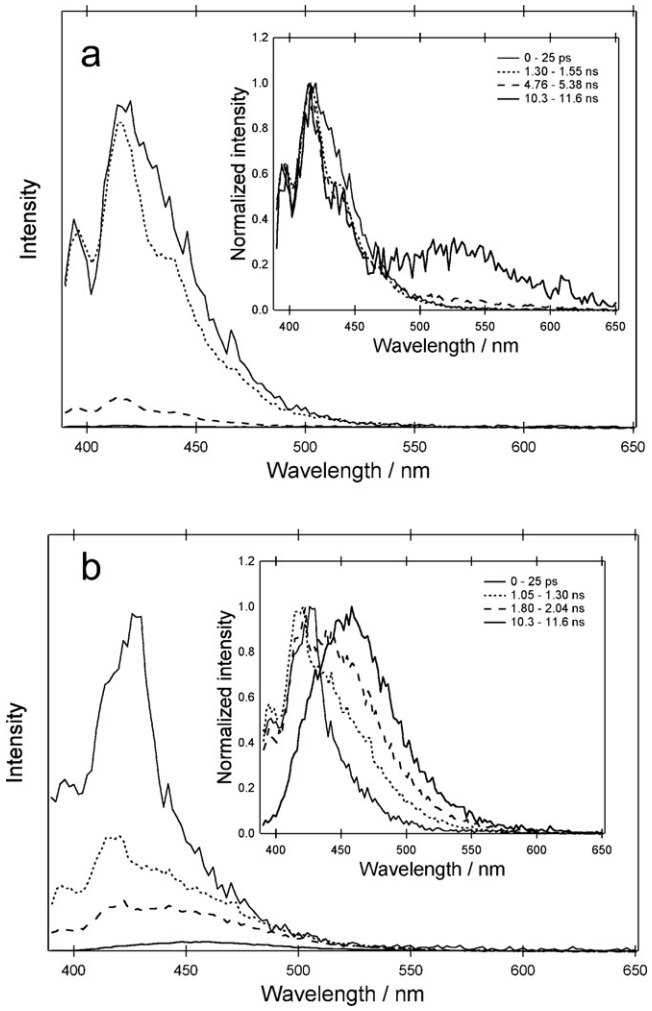

Fig. 5. Normalized time-resolved fluorescence spectra with peak intensities of (a) **wG1** and (b) **wG2** in 0.1 M KOH aqueous solution at room temperature. The excitation wavelength was 375 nm for all the experiments.

rings of anthracene gave fluorescences at 570 and 620 nm, respectively [23]. According to this deduction, the anthracene sites in both **wG1** and **wG2** that emit excimer fluorescence probably overlap by a single phenyl ring, but the angle of overlapped anthracene unit should be the difference between **wG1** and **wG2**.

Table 3 lists the fluorescence lifetimes at different KCl concentrations, which are consistent with the changes in the fluorescence spectra in Fig. 4. In the absence of KCl, we determined the lifetimes of **wG1** in 0.01 M KOH aqueous solution by fitting a multi-exponential function to be 0.08 ns (58%), 0.87 ns (40%), and 5.3 ns (2%). After the addition of KCl, the lifetime converged to 9.3 ns (100%), suggesting a single excimer conformation. On the other hand, the lifetime of **wG2** did not converge by the addition of KCl but became slightly longer than that before the KCl addition.

3.2. Time-resolved fluorescence spectra

Fig. 5a shows the time-resolved fluorescence spectra of **wG1** (3.1×10^{-6} M) in a 0.1 M KOH aqueous solution (left) and its superposition normalized at the emission maxima (inset). Fig. 2d shows the corresponding steady state spectrum (thin line). The emission spectrum observed after the excitation pulse from $t = 0$ to 0.25 ns was due to the anthracene monomer, while the spectrum observed after the excitation pulse of 10.3–11.5 ns consisted of one progression that we could assign to the excimer because the relative intensity of this emission band increased progressively in the time period of 1–10.3 ns. However, the lack of observation of the rise component indicated that the formation of the excimer within the dendrimer aggregates should be faster than the time resolved limit of the instrument. Fig. 5b depicts the time-resolved spectra of **wG2** (3.1×10^{-6} M) in the same measurement conditions. The time evolution of **wG2** was similar to that of **wG1**, but the excimer emission was more intense, agreeing with the steady state fluorescence spectra (see Fig. 2d, solid line).

4. Conclusions

In conclusion, the anthracene-cored poly(aryl ether) dendrimers formed aggregates at low concentrations in aqueous solution (2.0×10^{-5} M) to form micelles via the addition of KCl, results that were very different from the CMC of usual detergents ($\sim 10^{-2}$ M); the aggregate formation was highly dependent upon the generation. Furthermore, the results presented here are the first clear report of the observations of the excimer emission of anthracene in very low fluid solutions in which appropriate substituents were introduced. A comparison of the excimer fluorescence of **wG1** and **wG2** indicated that the different overlapping structures depended on the dendrimer generations. These findings of dendrimer aggregation revealed by photochemical techniques may be useful for developing new drug delivery systems using amphiphilic cone-shaped dendrimers.

Acknowledgement

This work was supported by a Grant-in-Aid for Scientific Research in a Priority Area "New Frontiers in Photochromism (No. 471) from the Ministry of Education, Culture, Sports, Science, and Technology (MEXT), Japan.

References

[1] D.A. Tomalia, A.M. Naylor, W.A. Goddard III, Angew. Chem. Int. Ed. Engl. 102 (1990) 119–157.
[2] J.M.J. Fréchet, Science 263 (1994) 1710–1715.
[3] D.A. Tomalia, P.R. Dvornic, Nature 372 (1994) 617–618.
[4] D.A. Tomalia, R. Esfand, Chem. Ind. (1997) 416–420.
[5] T. Emrick, J.M.J. Fréchet, Curr. Opin. Colloid Interface Sci. 4 (1999) 15–23.
[6] V. Percec, W.-D. Cho, M. Möller, S.A. Prokhorova, G. Ungar, D.J.P. Yeardley, J. Am. Chem. Soc. 122 (2000) 4249–4250.
[7] V. Percec, M. Glodde, T.K. Bera, Y. Miura, I. Shiyanovskaya, K.D. Singer, V.S.K. Balagurusamy, P.A. Heiney, I. Schnell, A. Rapp, H.-W. Spiess, S.D. Hudsonk, H. Duank, Nature 419 (2002) 384–387.
[8] M. Ogawa, A. Momotake, T. Arai, Tetrahedron Lett. 45 (2004) 8515–8518.
[9] P.F. Jones, M. Nicol, J. Chem. Phys. 48 (1968) 5440–5447.
[10] J.C. Amicangelo, W.R. Leenstra, J. Am. Chem. Soc. 125 (2003) 14698–14699.
[11] T. Costa, M.d.G. Miguel, B.r. Lindman, K. Schillén, J.S.r. Seixas de Melo, J. Phys. Chem. B 109 (2005) 11478–11492.
[12] J. Reichwagen, H. Hopf, A. Del Guerzo, J.-P. Desvergne, H. Bouas-Laurent, Org. Lett. 6 (2004) 1899–1902.
[13] T.H. Ghaddar, J.K. Whitesell, M.A. Fox, J. Phys. Chem. B 105 (2001) 8729–8731.
[14] R. Akatsuka, Y. Shinohara, T. Sato, Y. Nishimura, T. Arai, Bull. Chem. Soc. Jpn. 82 (2009) 242–248.
[15] S. Sengupta, N. Pal, Tetrahedron Lett. 43 (2002) 3517–3520.
[16] S. Sengupta, P. Purkayastha, Org. Biomol. Chem. 1 (2003) 436–440.
[17] L. Zhao, C. Li, Y. Zhang, X.-H. Zhu, J. Peng, Y. Cao, Macromol. Rapid. Commun. 27 (2006) 914–920.
[18] Y. Takaguchi, T. Tajima, K. Ohta, J. Motoyoshiya, H. Aoyama, Chem. Lett. (2000) 1388–1389.
[19] M. Fujitsuka, O. Ito, Y. Takaguchi, T. Tajima, K. Ohta, J. Motoyoshiya, H. Aoyama, Bull. Chem. Soc. Jpn. 76 (2003) 743–747.
[20] Y. Nishimura, M. Kamada, M. Ikegami, R. Nagahata, T. Arai, J. Photochem. Photobiol. A: Chem. 178 (2006) 150.
[21] T. Hayashi, N. Mataga, Y. Sakata, S. Misumi, M. Morita, J. Tanaka, J. Am. Chem. Soc. 98 (1976) 5910–5913.
[22] M. Itoh, K. Fuke, S. Kobayashi, J. Chem. Phys. 72 (1980) 1417–1418.
[23] Z. Lin, S. Priyadarshy, A. Bartko, D.H. Waldeck, J. Photochem. Photobiol. A: Chem. 110 (1997) 131–139.